Collective phenomena and shell structure far from stability

Frédéric Nowacki[1]

[1] Strasbourg-Madrid Shell-Model collaboration

What are the data needed to constrain and refine models ?

THE DRAMA:

What are the data needed to constrain and refine models ?

THE DRAMA:

- Theorists here in the room :

  “None ! We don’t need any !”

What are the data needed to constrain and refine models ?

THE DRAMA:

- Theorists here in the room :

  "None ! We don't need any !"

- Experimentalists here in the room :

  "All of them ! Let's measure all of them !"

What are the data needed to constrain and refine models ?

THE DRAMA:

- Theorists here in the room :

  "None ! We don't need any !"

- Experimentalists here in the room :

  "All of them ! Let's measure all of them !"

Fortunately, life has made us more reasonable ... and things more simple !

Shell Model: Physics Goals

Collective excitations:

- Deformation, Superdeformation,

Dipole/M1 resonances

- Superfluidity
- Symmetries

Weak processes:

- β decay
- $\beta\beta$ decay

$$[T^{0\nu}_{1/2}(0^+ \rightarrow 0^+)]^{-1} = G_{0\nu}|M^{0\nu}|^2 \langle m_\nu \rangle^2$$

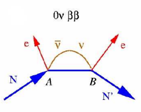

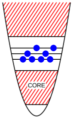

- define Effective Interaction
- $\mathcal{H}_{\text{eff}}\Psi_{\text{eff}} = E\Psi_{\text{eff}}$
- build and diagonalize Energy matrix

Shell evolution far from stability:

- Vanishing of shell closures
- New magic numbers

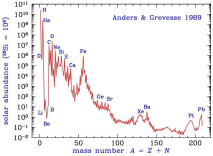

Ab Initio calculations:

- Chiral EFT realistic interactions
- 3N forces

Shell Model: Giant Computations

- exponential growth of basis dimensions:

$$D \sim \binom{d_\pi}{p} \cdot \binom{d_\nu}{n}$$

In *pf* shell :

^{48}Cr 1,963,461

^{56}Ni **1,087,455,228**

In *pf-sdg* space :

^{78}Ni **210,046,691,518**

- Actual limits in limits in giant diagonalizations: **0.2 10^{12}** for ^{114}Sn core excitations

- Some of the largest diagonalizations ever are performed in Strasbourg with relatively modest computationnal ressources:

  Phys. Rev. C82 (2010) 054301, ibidem 064304

  - m scheme ANTOINE code
  - coupled scheme NATHAN code

E. Caurier et al., Rev. Mod. Phys. 77 (2005) 427; ANTOINE website

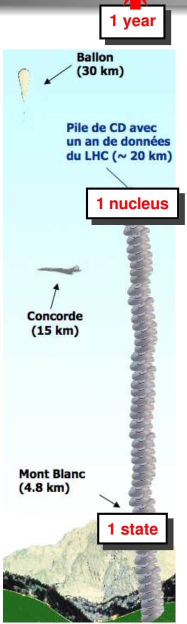

- Largest matrices up to now contain up to $\sim$ **10^{14}** non-zero matrix elements.

- This would require more than 1,000,000 CD-ROM's to store the information for a single matrix !

- They cannot be stored on hard disk and are computed on the fly.

Discrete Non-Orthogonal Shell Model

Generator Coordinate Method: $|\Psi_{\text{eff}}\rangle = \sum_i f_i |\Phi_i\rangle$

1) Deformed Hartree-Fock (HF) Slater determinants

2) Restoration of rotational symmetry

3) Mixing of shapes:

$|\Psi_{\text{eff}}\rangle =$ 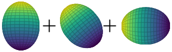 $\cdots$

Basis Truncation Method

? *choice of relevant deformed Hartree-Fock states*

- **E. Caurier's Minimization Technique**:

(E. Caurier, Proc. on GCM, BLG report **484** (1975))

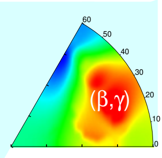

◇ Based on the variational principle

◇ Minimization of the energy of given states $\{J^\pi\}$

- **Iterative procedure**:

$\Phi_1 \rightarrow (\Phi_1, \Phi_2) \rightarrow (\Phi_1, \Phi_2, \Phi_3) \cdots$

$N = 1$ $\quad N = 2$ $\quad N = 3$

Discrete Non-Orthogonal Shell Model

Generator Coordinate Method: $|\Psi_{\rm eff}\rangle = \sum_i f_i |\Phi_i\rangle$

1) Deformed Hartree-Fock (HF) Slater determinants

2) Restoration of rotational symmetry

3) Mixing of shapes:

$|\Psi_{\rm eff}\rangle =$ 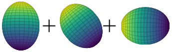 $\cdots$

Intrinsic/Laboratory Description

- **Deformation structure of nuclear states**: $\{J^\pi_\alpha\}$, $q = (\beta, \gamma)$

$$M^{(J)}_\alpha(q, K) = \sum_{q', K'} [\hat{N}^{1/2}]^{(J)}_{K'K}(q', q)\, f^{(J)}_\alpha(q', K')$$

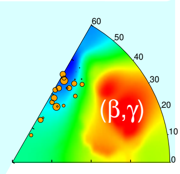

◇ Probability of a configuration (β, γ):

$$P^{(J)}_\alpha(q) = \sum_K |M^{(J)}_\alpha(q, K)|^2$$

- **particle-hole interpretation**:

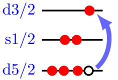

M**-scheme**

- **K–quantum numbers**:

$$P^{(J)}_\alpha(K) = \sum_q |M^{(J)}_\alpha(q, K)|^2$$

Discrete Non-Orthogonal Shell Model

PHYSICAL REVIEW C **105**, 054314 (2022)

Nuclear structure within a discrete nonorthogonal shell model approach: New frontiers

D. D. Dao and F. Nowacki
Université de Strasbourg, CNRS, IPHC UMR7178, 23 rue du Loess, F-67000 Strasbourg, France

(Received 8 March 2022; accepted 6 May 2022; published 23 May 2022)

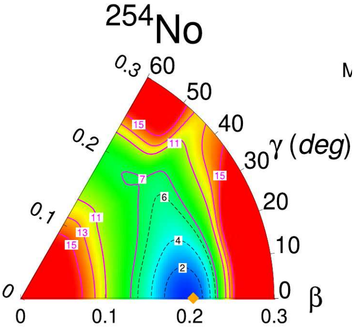

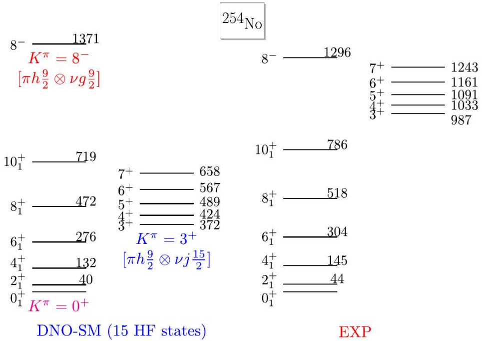

First “SM” calculations for superheavies !!!

Landscape of medium mass nuclei

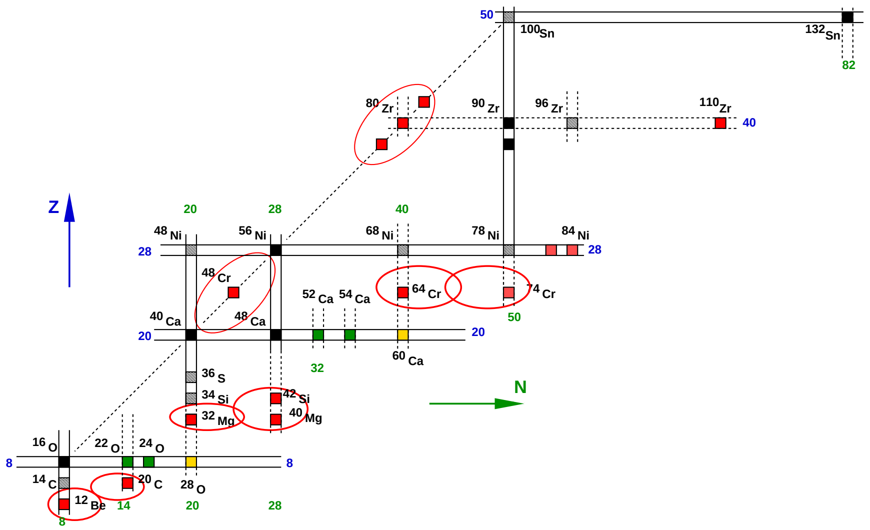

Landscape of medium mass nuclei

- New gaps: ^{24}O, ^{48}Ni, ^{54}Ca, ^{78}Ni, ^{100}Sn
- Vanishing of shell closure: ^{12}Be, ^{32}Mg, ^{42}Si, ^{64}Cr, ^{80}Zr ...
- Island of deformation around A$\sim$ 32, A$\sim$ 64
- Low-lying dipole excitations in Ne, Ni isotopes

- Variety of phenomena dictated by shell structure
- Close connection between collective behaviour and underlying shell structure
- Interplay between
  - Monopole field (spherical mean field)
  - Multipole correlations (pairing, Q.Q, ...)

“Pairing plus Quadrupole propose, Monopole disposes”
A. Zuker, Coherent and Random Hamiltonians, CRN Preprint 1994

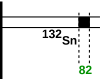

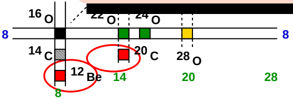

Development of deformation at N=8,20,40,70

- Magic numbers are associated to enegy gaps in the spherical mean field. Therefore, to promote particles above the Fermi levels costs energy
- However some intruders configurations can overwhelm their loss of monopole energy with their huge gain in correlation energy
- Several examples of this phenomenon exist in stable magic nuclei (as in ^{40}Ca nucleus) in the form of coexisting spherical, deformed and superdeformed states in a very narrow energy range
- At the very neutron rich or very proton rich edges, the T=0 and T=1 channels of the effective nuclear interaction weight very differently than they do at the stability line. Therefore the effective single particle structure may suffer important changes, leading in some cases to the vanishing of established shell closures or to the appearance of new ones

Fig. 40. Schematic view of the valence spaces at N = 8, 20, 40 and 70. The intruder configurations that develop quadrupole collectivity are highlighted.

Development of deformation at N=8,20,40,70

F. Nowacki, A. Obertelli and A. Poves — Progress in Particle and Nuclear Physics 120 (2021) 103866

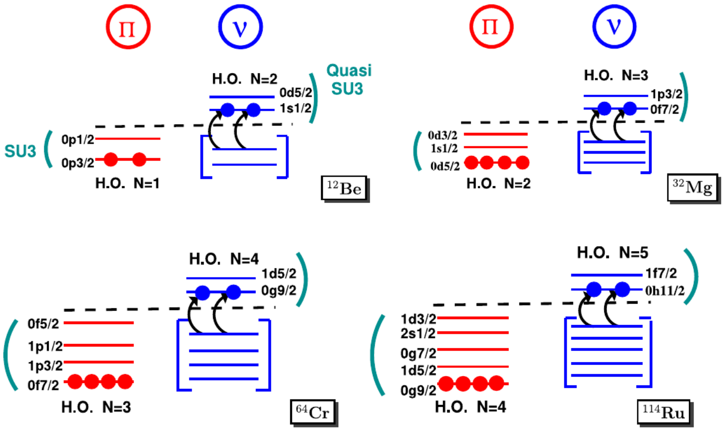

Fig. 40. Schematic view of the valence spaces at N = 8, 20, 40 and 70. The intruder configurations that develop quadrupole collectivity are highlighted.

Development of deformation at N=14,28,50,82

F. Nowacki, A. Obertelli and A. Poves Progress in Particle and Nuclear Physics 120 (2021) 103866

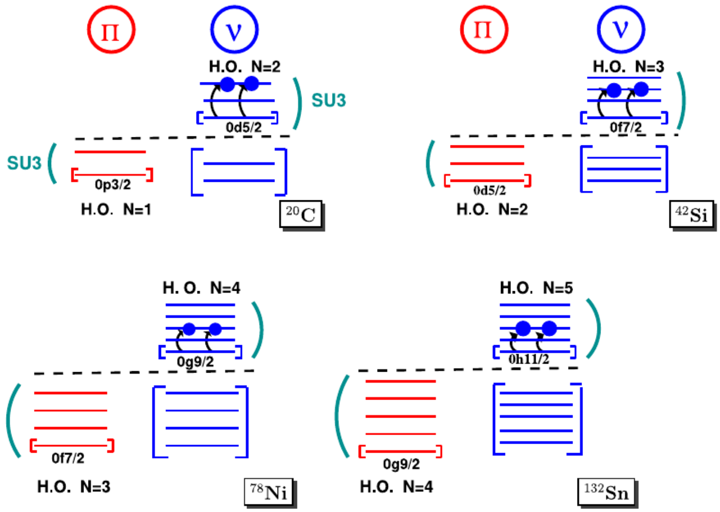

Fig. 41. Schematic view of the valence spaces at N = 14, 28, 50 and 82. The intruder configurations that develop quadrupole collectivity are highlighted.

The nuclear interaction: the complex view

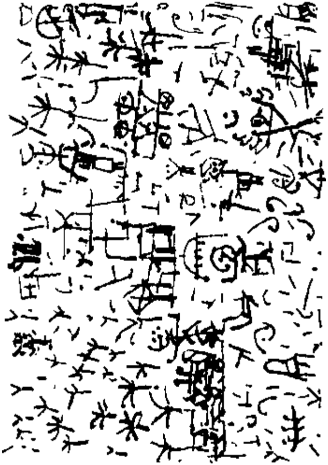

P. Klee, art

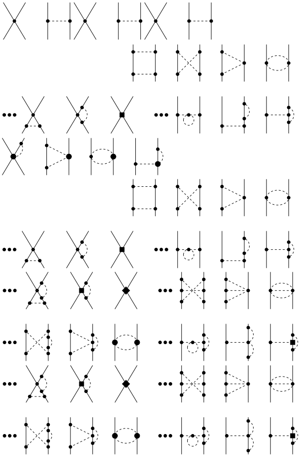

E. Epelbaum, physics

The nuclear interaction: the simple view

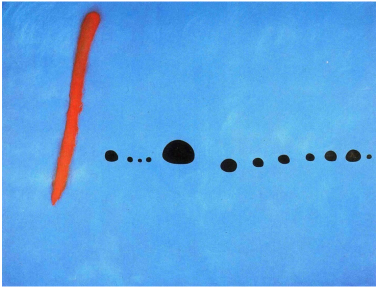

J. Miro, art

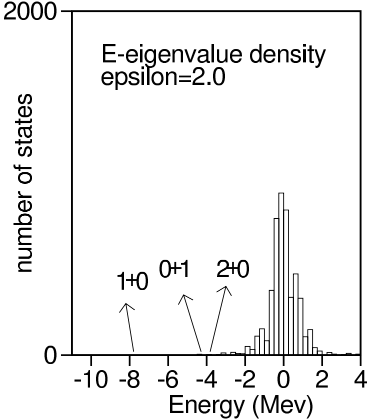

A. Zuker, physics

Separation of the effective Hamiltonian
Monopole and multipole

From the work of M. Dufour and A. Zuker (PRC 54 1996 1641)
Separation theorem:

Any effective interaction can be split in two parts:

$$H = H_{monopole} + H_{multipole}$$

$H_{monopole}$: *spherical mean-field*

☞responsible for the global saturation properties and for the evolution of the spherical single particle levels.

$H_{multipole}$: *correlator*

☞ pairing, quadrupole, octupole...

Important property:

$$\langle CS \pm 1 | H | CS \pm 1 \rangle \ = \ \langle CS \pm 1 | H_{monopole} | CS \pm 1 \rangle$$

Multipole Hamiltonian

$H_{multipole}$ can be written in two representations, particle-particle and particle-hole. Both can be brought into a diagonal form. When this is done, it comes out that only a few terms are coherent, and those are the simplest ones:

- $L = 0$ isovector and isoscalar pairing
- Elliott's quadrupole
- $\vec{\sigma}\vec{\tau} \cdot \vec{\sigma}\vec{\tau}$
- Octupole and hexadecapole terms of the type $r^{\lambda} Y_{\lambda} \cdot r^{\lambda} Y_{\lambda}$

Besides, they are universal (all the realistic interactions give similar values) and scale simply with the mass number

	pp(JT)			ph($\lambda\tau$)			
	10	01	21	20	40	10	11
KB	-5.83	-4.96	-3.21	-3.53	-1.38	+1.61	+3.00
USD-A	-5.62	-5.50	-3.17	-3.24	-1.60	+1.56	+2.99
CCEI	-6.79	-4.68	-2.93	-3.40	-1.39	+1.21	+2.83
NN+NNN-MBPT	-6.40	-4.36	-2.91	-3.28	-1.23	+1.10	+2.43
NN-MBPT	-6.06	-4.38	-2.92	-3.35	-1.31	+1.03	+2.49

Multipole Hamiltonian

$H_{multipole}$ can be written in two representations, particle-particle
and pa
When
cohere

- L =
- Ell
- $\vec{\sigma}\vec{\tau}$
- Oc

Beside
similar

KB
USD
CCE
NN+
NN-

- **Pairing regime: spherical nuclei**

  ground state = pairs of like-particles coupled at J=0 (seniority v=0)

  2^+ state (break of pair; v=2) at high energy

  superfluid nucleus:

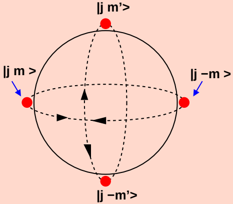

  Typical example: **Tin isotopes**

- **Quadrupole regime: deformed nuclei**

  prolate nucleus:

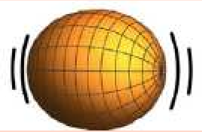

  Typical example: **open shell N=Z nuclei**

Multipole Hamiltonian

$H_{multipole}$ can be written in two representations, particle-particle and particle-hole. Both can be brought into a diagonal form. When this is done, it comes out that only a few terms are coherent, and those are the simplest ones:

- $L = 0$ isovector and isoscalar pairing
- Elliott's quadrupole
- $\vec{\sigma}\vec{\tau} \cdot \vec{\sigma}\vec{\tau}$
- Octupole and hexadecapole terms of the type $r^{\lambda} Y_{\lambda} \cdot r^{\lambda} Y_{\lambda}$

Besides, they are universal (all the realistic interactions give similar values) and scale simply with the mass number

	pp(JT)			ph($\lambda\tau$)			
	10	01	21	20	40	10	11
KB	-5.83	-4.96	-3.21	-3.53	-1.38	+1.61	+3.00
USD-A	-5.62	-5.50	-3.17	-3.24	-1.60	+1.56	+2.99
CCEI	-6.79	-4.68	-2.93	-3.40	-1.39	+1.21	+2.83
NN+NNN-MBPT	-6.40	-4.36	-2.91	-3.28	-1.23	+1.10	+2.43
NN-MBPT	-6.06	-4.38	-2.92	-3.35	-1.31	+1.03	+2.49

Multipole Hamiltonian

$H_{multipole}$ can be written in two representations, particle-particle and particle-hole. Both can be brought into a diagonal form. When this is done, it comes out that only a few terms are coherent, and those are the simplest ones:

- $L = 0$ isovector and isoscalar pairing
- Elliott's quadrupole
- $\vec{\sigma}\vec{\tau} \cdot \vec{\sigma}\vec{\tau}$
- Octupole and hexadecapole terms of the type $r^{\lambda} Y_{\lambda} \cdot r^{\lambda} Y_{\lambda}$

Besides, they are universal (all the realistic interactions give similar values) and scale simply with the mass number

	pp(JT)		ph($\lambda\tau$)				
	10	01	21	20	40	10	11
KB	-5.83	-4.96	3.21	-3.53	-1.38	+1.61	+3.00
USD-A	-5.62	-5.50	3.17	-3.24	-1.60	+1.56	+2.99
CCEI	-6.79	-4.68	2.93	-3.40	-1.39	+1.21	+2.83
NN+NNN-MBPT	-6.40	-4.36	2.91	-3.28	-1.23	+1.10	+2.43
NN-MBPT	-6.06	-4.38	2.92	-3.35	-1.31	+1.03	+2.49

Multipole Hamiltonian

$H_{multipole}$ can be written in two representations, particle-particle and particle-hole. Both can be brought into a diagonal form. When this is done, it comes out that only a few terms are coherent, and those are the simplest ones:

- $L = 0$ isovector and isoscalar pairing
- Elliott's quadrupole
- $\vec{\sigma}\vec{\tau} \cdot \vec{\sigma}\vec{\tau}$
- Octupole and hexadecapole terms of the type $r^{\lambda} Y_{\lambda} \cdot r^{\lambda} Y_{\lambda}$

Besides, they are universal (all the realistic interactions give similar values) and scale simply with the mass number

	pp(JT)			ph(λτ)			
	10	01	21	20	40	10	11
KB	-5.83	-4.96	-3.21	-3.53	-1.38	+1.61	+3.00
USD-A	-5.62	-5.50	-3.17	-3.24	-1.60	+1.56	+2.99
CCEI	-6.79	-4.68	-2.93	-3.40	-1.39	+1.21	+2.83
NN+NNN-MBPT	-6.40	-4.36	-2.91	-3.28	-1.23	+1.10	+2.43
NN-MBPT	-6.06	-4.38	-2.92	-3.35	-1.31	+1.03	+2.49

Landscape of medium mass nuclei

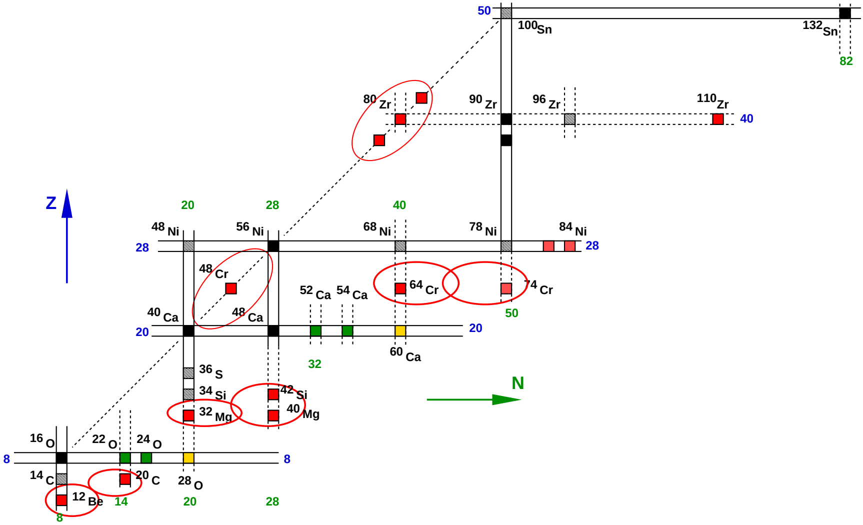

Playground

In the valence space of two major shells

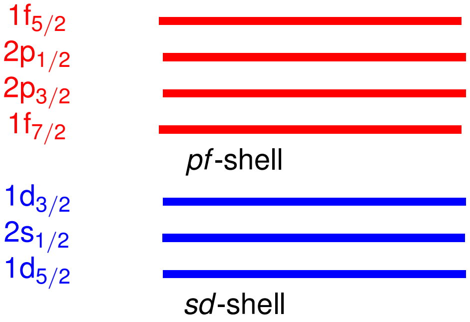

EFFECTIVE INTERACTION: SDPF-U-MIX (update 2020)

Island of Inversion: Trends

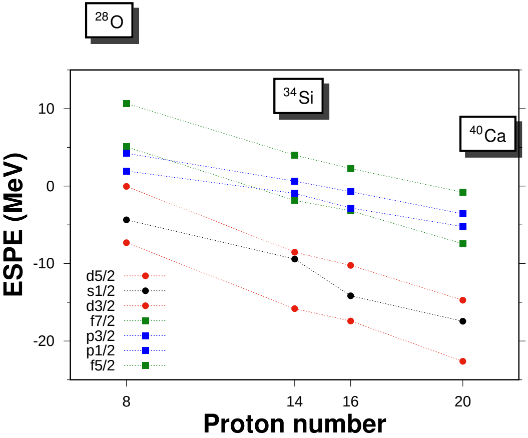

- At the neutron drip line, the ESPE's of ^{28}O are completely at variance with those of ^{40}Ca at the stability valley. The change from the standard ESPE's of ^{16}O to the anomalous ones in ^{28}O is totally due to the interactions of *sd* shell neutrons among themselves

- Notice that the *sd* shell orbits remain always below th *pf* shell with the $\nu 0f_{\frac{7}{2}}$ and $\nu 0p_{\frac{3}{2}} - 0p_{\frac{1}{2}}$ orbitals DO get inverted

- The monopole part of the neutron-proton interaction restores the N=20 shell gap when the valley of stability is approached

- Spin-Tensor decomposition shows it is mainly a Central and Tensor effect

Islands Of Inversion: Trends

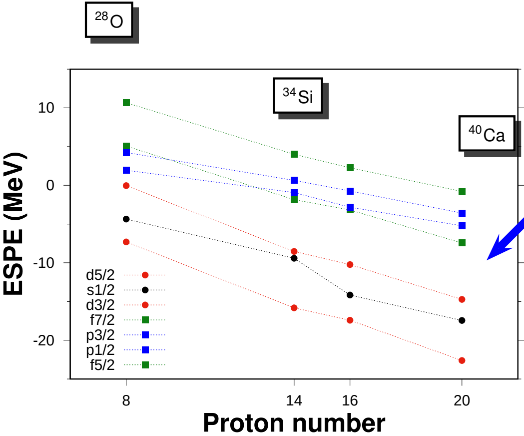

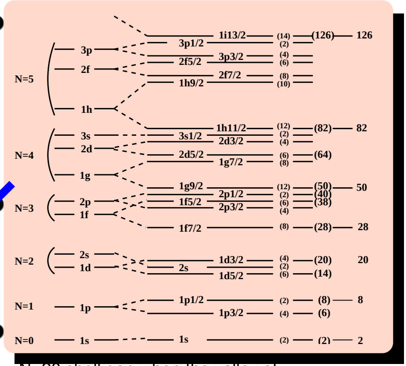

- N=20 shell gap when the valley of stability is approached

- Spin-Tensor decomposition shows it is mainly a Central and Tensor effect

Further away from Stability

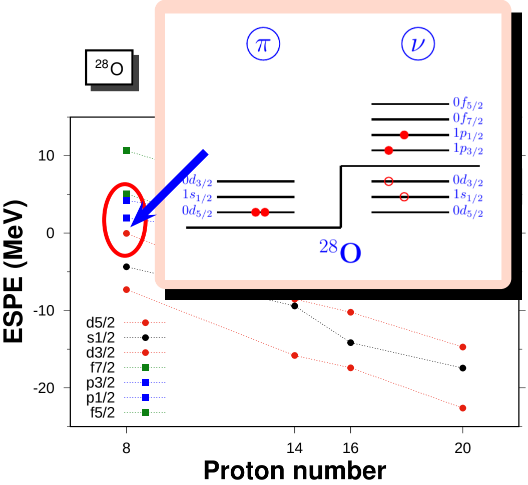

- At the neutron drip line, the ESPE's of ^{28}O are completely at variance with those of ^{40}Ca at the stability valley. The change from the standard ESPE's of ^{16}O to the anomalous ones in ^{28}O is totally due to the interactions of *sd* shell neutrons among themselves

- Notice that the *sd* shell orbits remain always below th *pf* shell with the $\nu 0f_{\frac{7}{2}}$ and $\nu 0p_{\frac{3}{2}} - 0p_{\frac{1}{2}}$ orbitals DO get inverted

- The monopole part of the neutron-proton interaction restores the N=20 shell gap when the valley of stability is approached

- Shell Evolution favors natural geometry for low-lying M1 excitations

$$\begin{matrix} \nu 1s_{\frac{1}{2}} \\ \nu 0d_{\frac{3}{2}} \end{matrix} \otimes \begin{matrix} \nu 1p_{\frac{3}{2}} \\ \nu 1p_{\frac{1}{2}} \end{matrix}$$

Island of Inversion: Trends

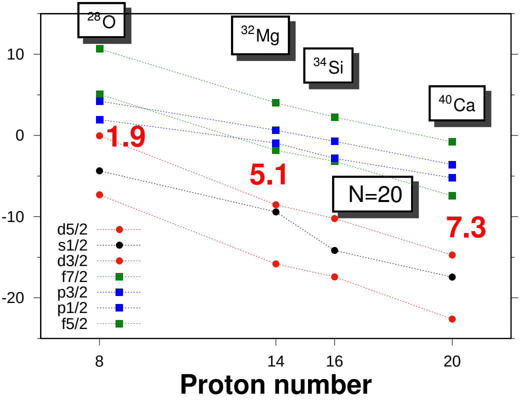

- At the neutron drip line, the ESPE's of ^{28}O are completely at variance with those of ^{40}Ca at the stability valley. The change from the standard ESPE's of ^{16}O to the anomalous ones in ^{28}O is totally due to the interactions of *sd* shell neutrons among themselves

- Notice that the *sd* shell orbits remain always below th *pf* shell with the $\nu 0f_{\frac{7}{2}}$ and $\nu 0p_{\frac{3}{2}} - 0p_{\frac{1}{2}}$ orbitals DO get inverted

- The monopole part of the neutron-proton interaction restores the N=20 shell gap when the valley of stability is approached

- Spin-Tensor decomposition shows it is mainly a Central and Tensor effect

Inverse shape coexistence Shell closure in ^{32}Mg

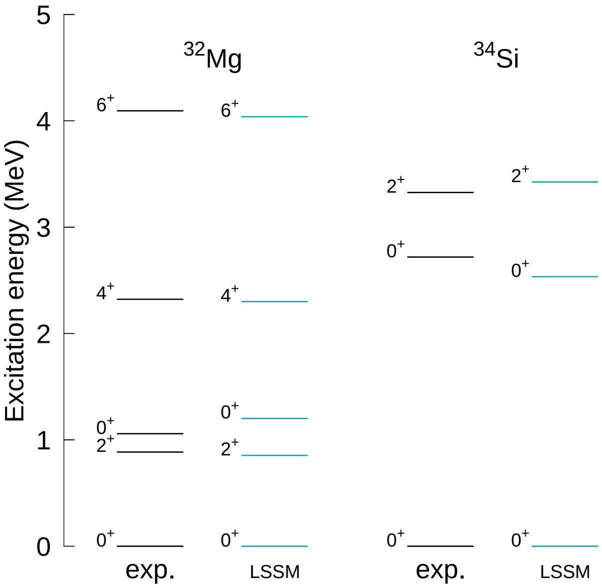

Merging of IOIs at N=20 and N=28

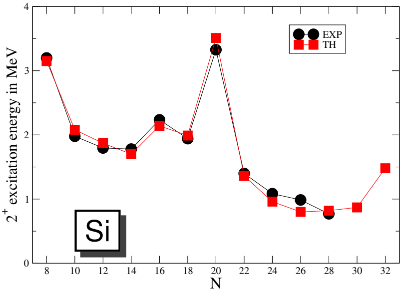

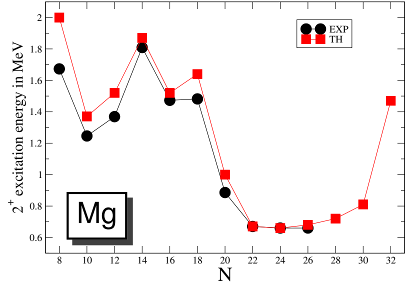

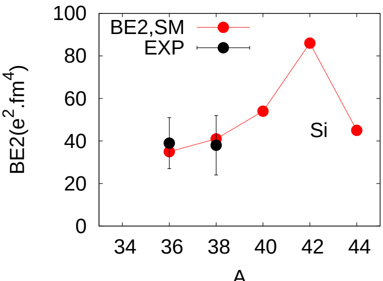

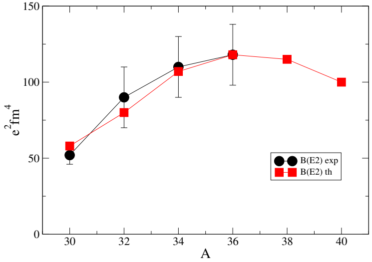

At the drip line

RAPID COMMUNICATIONS

PHYSICAL REVIEW C **85**, 011302(R) (2012)

Low-lying neutron fp-shell intruder states in ^{27}Ne

S. M. Brown,[1] W. N. Catford,[1] J. S. Thomas,[1] B. Fernández-Domínguez,[2,3] N. A. Orr,[2] M. Labiche,[4] M. Rejmund,[5] N. L. Achouri,[2] H. Al Falou,[2] N. I. Ashwood,[6] D. Beaumel,[7] Y. Blumenfeld,[7] B. A. Brown,[8] R. Chapman,[9] M. Chartier,[3] N. Curtis,[6] G. de France,[5] N. de Sereville,[7] F. Delaunay,[2] A. Drouart,[10] C. Force,[5] S. Franchoo,[7] J. Guillot,[7] P. Haigh,[6] F. Hammache,[7] V. Lapoux,[10] R. C. Lemmon,[4] A. Leprince,[2] F. Maréchal,[7] X. Mougeot,[10] B. Mouginot,[7] L. Nalpas,[10] A. Navin,[5] N. P. Patterson,[1] B. Pietras,[3] E. C. Pollacco,[10] A. Ramus,[7] J. A. Scarpaci,[7] I. Stefan,[7] and G. L. Wilson[1]

LOW-LYING NEUTRON fp-SHELL INTRUDER STATES ...

TABLE I. Comparison between experimental and calculated (see text) excitation energies and spectroscopic factors for states in ^{27}Ne. Experimental excitation energies are from [10] except for the 1.74-MeV state (present work). For C^2S, the errors include uncertainties from the reaction model.

J^π	$E^*_{\rm exp}$ (MeV)	$E^*_{WBP\text{-}M}$ (MeV)	C^2S Ref. [10]	C^2S Present	C^2S WBP-M
$3/2^+$	0	0	0.2(2)	0.42(22)	0.63
$3/2^-$	0.765	0.809	0.6(2)	0.64(33)	0.67
$1/2^+$	0.885	0.869	0.3(1)	0.17(14)	0.17
$7/2^-$	1.74	1.686	–	0.35(10)	0.40

At the neutron drip line, the ESPE's of ^{28}O are completely at variance with those of ^{40}Ca at the stability valley. The change from the standard ESPE's of ^{16}O to the anomalous ones in ^{28}O is totally due to the interactions of *sd* shell neutrons among themselves

- Notice that the *sd* shell orbits remain always below th *pf* shell with the $\nu 0f_{\frac{7}{2}}$ and $\nu 0p_{\frac{3}{2}} - 0p_{\frac{1}{2}}$ orbitals DO get inverted
- The monopole part of the neutron-proton interaction restores the N=20 shell gap when the valley of stability is approached
- Evidence for shell inversion towards ^{28}O

At the drip line

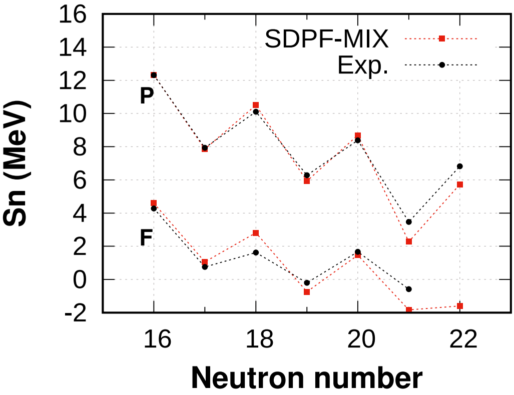

Nowacki/Poves 2014

- At the neutron drip line, the ESPE's of ^{28}O are completely at variance with those of ^{40}Ca at the stability valley. The change from the standard ESPE's of ^{16}O to the anomalous ones in ^{28}O is totally due to the interactions of *sd* shell neutrons among themselves
- Notice that the *sd* shell orbits remain always below th *pf* shell with the $\nu 0f_{\frac{7}{2}}$ and $\nu 0p_{\frac{3}{2}} - 0p_{\frac{1}{2}}$ orbitals DO get inverted
- The monopole part of the neutron-proton interaction restores the N=20 shell gap when the valley of stability is approached
- "ill" behaviour mainly due to ^{38}P separation energy

At the drip line

PHYSICAL REVIEW LETTERS **124,** 152502 (2020)

Extending the Southern Shore of the Island of Inversion to ^{28}F

A. Revel,[1,2] O. Sorlin,[1] F. M. Marqués,[2] Y. Kondo,[3] J. Kahlbow,[4,5] T. Nakamura,[3] N. A. Orr,[2] F. Nowacki,[6,7]

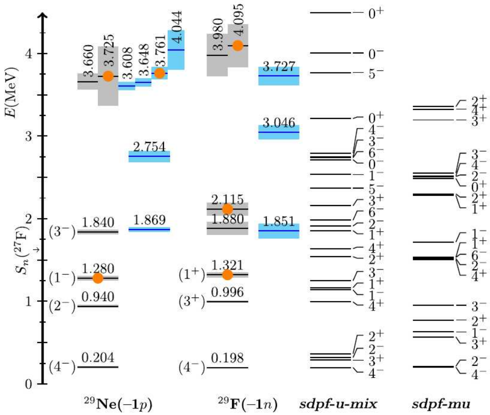

- At the neutron drip line, the ESPE's of ^{28}O are completely at variance with those of ^{40}Ca at the stability valley.
- Notice that the *sd* shell orbits remain always below th *pf* shell with the $\nu 0f_{\frac{7}{2}}$ and $\nu 0p_{\frac{3}{2}} - 0p_{\frac{1}{2}}$ orbitals DO get inverted
- Recent evidence for intruder states in ^{28}F low-lying spectrum
- In addition, extraction of 80% of "l=1" content in the GS

At the drip line

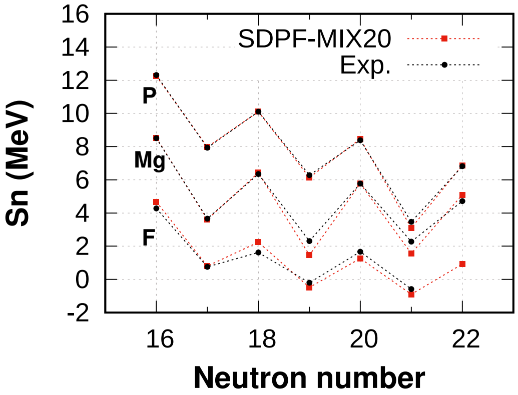

Nowacki/Poves 2020

- At the neutron drip line, the ESPE's of ^{28}O are completely at variance with those of ^{40}Ca at the stability valley. The change from the standard ESPE's of ^{16}O to the anomalous ones in ^{28}O is totally due to the interactions of *sd* shell neutrons among themselves

- Notice that the *sd* shell orbits remain always below th *pf* shell with the $\nu 0f_{\frac{7}{2}}$ and $\nu 0p_{\frac{3}{2}} - 0p_{\frac{1}{2}}$ orbitals DO get inverted

- The monopole part of the neutron-proton interaction restores the N=20 shell gap when the valley of stability is approached

- **New ^{30}F data from NeuLAND-SAMOURAI collaboration (J. Kahlbow phD work, submitted)**

- ^{38}P separation energy + $p_{3/2}$-$f_{7/2}$ splitting matches Fluorine chain S_n trend

Landscape of medium mass nuclei

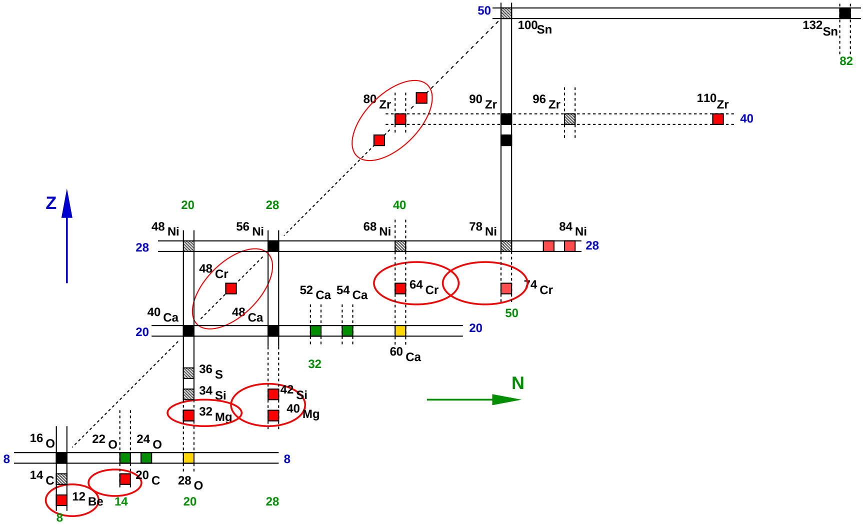

Island of inversion at N=40, an old story: 1996

The Physics around the doubly-magic ^{78}Ni Nucleus

Leuven, Belgium
November 4-5, 1996

A. Poves

^{64}Cr

$$g(0ph - 2ph) = 5.70$$
$$g(0ph - 4ph) = 8.30$$

$Q = -9.0\ b^2$

$BE2 = 19.8\ b^4$

$cs < 1\%$

$n(d_{5/2}) = 1.1$

$$\frac{E(4^+)}{E(2^+)} = 2.7 \qquad \left[\frac{E(4^+)}{E(2^+)} = (3.2)\,(3.4)\right]$$

in the intruder configurations.

A SITUATION THAT REMINDS WHAT IS KNOWN AT N=20 FFS.

More recent experimental information

RAPID COMMUNICATIONS

PHYSICAL REVIEW C **81**, 051304(R) (2010)

Collectivity at $N = 40$ in neutron-rich ^{64}Cr

A. Gade,[1,2] R. V. F. Janssens,[3] T. Baugher,[1,2] D. Bazin,[1] B. A. Brown,[1,2] M. P. Carpenter,[3] C. J. Chiara,[3,4] A. N. Deacon,[5] S. J. Freeman,[5] G. F. Grinyer,[1] C. R. Hoffman,[3] B. P. Kay,[3] F. G. Kondev,[6] T. Lauritsen,[3] S. McDaniel,[1,2] K. Meierbachtol,[1,7] A. Ratkiewicz,[1,2] S. R. Stroberg,[1,2] K. A. Walsh,[1,2] D. Weisshaar,[1] R. Winkler,[1] and S. Zhu[3]

[1]*National Superconducting Cyclotron Laboratory, Michigan State University, East Lansing, Michigan 48824, USA*

[2]*Department of Physics and Astronomy, Michigan State University, East Lansing, Michigan 48824, USA*

[3]*Physics Division, Argonne National Laboratory, Argonne, Illinois 60439, USA*

RAPID COMMUNICATIONS

PHYSICAL REVIEW C **81**, 061301(R) (2010)

Onset of collectivity in neutron-rich Fe isotopes: Toward a new island of inversion?

J. Ljungvall,[1,2,3] A. Görgen,[1] A. Obertelli,[1] W. Korten,[1] E. Clément,[2] G. de France,[2] A. Bürger,[4] J.-P. Delaroche,[5] A. Dewald,[6] A. Gadea,[7] L. Gaudefroy,[5] M. Girod,[5] M. Hackstein,[6] J. Libert,[8] D. Mengoni,[9] F. Nowacki,[10] T. Pissulla,[6] A. Poves,[11] F. Recchia,[12] M. Rejmund,[2] W. Rother,[6] E. Sahin,[12] C. Schmitt,[2] A. Shrivastava,[2] K. Sieja,[10] J. J. Valiente-Dobón,[12] K. O. Zell,[6] and M. Zielińska[13]

[1]*CEA Saclay, IRFU, Service de Physique Nucléaire, F-91191 Gif-sur-Yvette, France*

[2]*GANIL, CEA/DSM-CNRS/IN2P3, Bd Henri Becquerel, BP 55027, F-14076 Caen, France*

SM framework

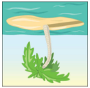

Island of inversion around ^{64}Cr

S. Lenzi, F. Nowacki, A. Poves and K. Sieja

Phys. Rev. C82, 054301, 2010

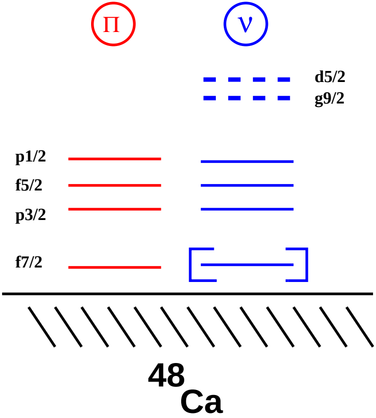

LNPS interaction:

- based on realistic TBME
- new fit of the pf shell (KB3GR, E. Caurier)
- monopole corrections
- $g_{9/2}$-$d_{5/2}$ gap now constrained to 2.5 Mev in ^{68}Ni

Calculations:

- Up to $14\hbar\omega$ excitations across Z=28 and N=40 gaps
- Matrix diagonalizations up to 2.10^{10}
- m-scheme code ANTOINE (non public parallel version)

Triple coexistence in ^{68}Ni

- at first approximation, ^{68}Ni has a double closed shell structure for GS
- But low lying structure much more complex
- three coexisting 0^+ states appear between 0 and $\sim$ 2.5 MeV
- new location of 0_2^+ state !
  Configuration mixing and relative transition rates between low-spin states in ^{68}Ni:
  F. Recchia et al.
  Phys. Rev. **C88**, 041302(R) (2013)
- prediction of very low-lying superdeformed band ($\beta_2 \sim 0.4$) of $6p6h$ nature!
  •S. Lenzi et al.
  Phys. Rev. **C82**, 054301 (2010)
  •A. Dijon et al.
  Phys. Rev. **C85**, 0311301(R) (2012)

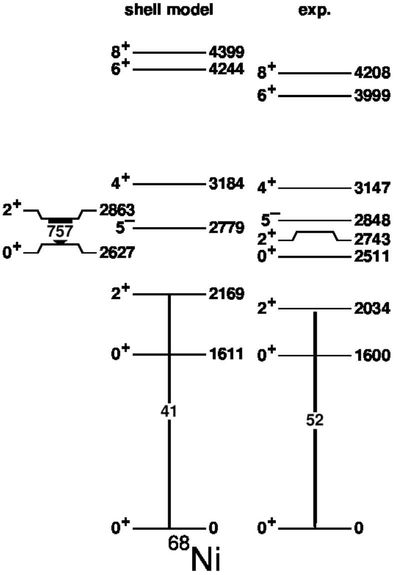

Shape transition at N=40

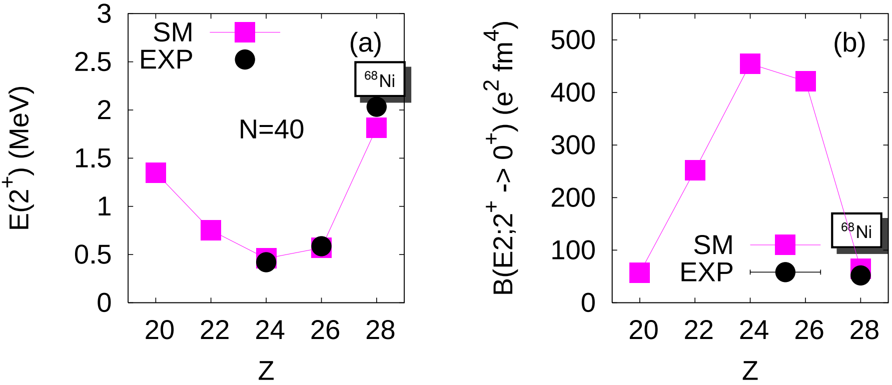

Nucleus	$\nu g_{9/2}$	$\nu d_{5/2}$	configuration
^{68}Ni	0.98	0.10	0p0h(51%)
^{66}Fe	3.17	0.46	4p4h(26%)
^{64}Cr	3.41	0.76	6p6h(23%)
^{62}Ti	3.17	1.09	4p4h(48%)

Shape transition at N=40

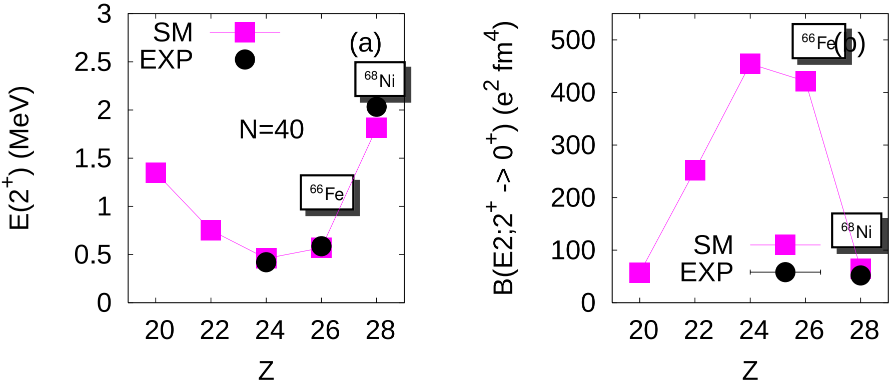

Nucleus	$\nu g_{9/2}$	$\nu d_{5/2}$	configuration
^{68}Ni	0.98	0.10	0p0h(51%)
^{66}Fe	3.17	0.46	4p4h(26%)
^{64}Cr	3.41	0.76	6p6h(23%)
^{62}Ti	3.17	1.09	4p4h(48%)

Shape transition at N=40

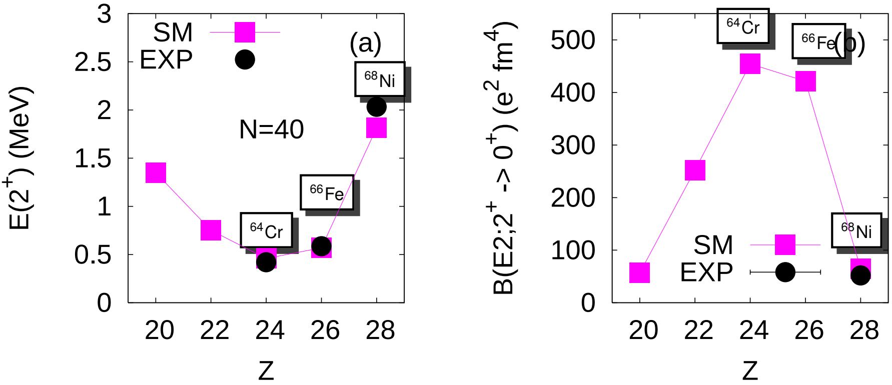

Nucleus	$\nu g_{9/2}$	$\nu d_{5/2}$	configuration
^{68}Ni	0.98	0.10	0p0h(51%)
^{66}Fe	3.17	0.46	4p4h(26%)
^{64}Cr	3.41	0.76	6p6h(23%)
^{62}Ti	3.17	1.09	4p4h(48%)

Neutron effective single particle energies

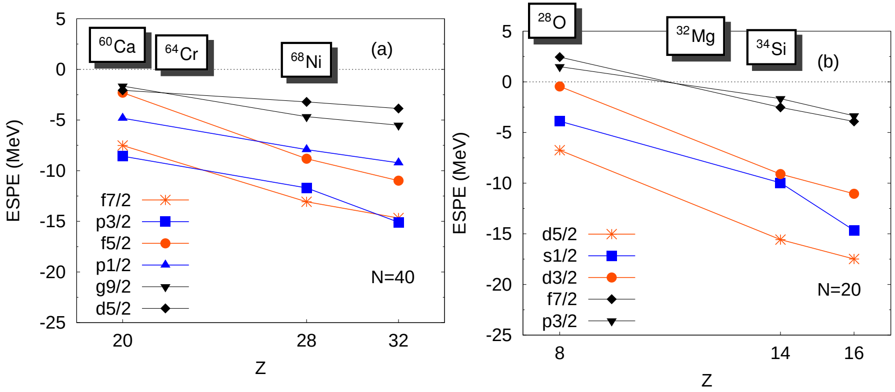

- reduction of the $\nu f_{5/2}$-$g_{9/2}$ gap with removing $f_{7/2}$ protons
- proximity of the quasi-SU3 partner $d_{5/2}$
- inversion of $d_{5/2}$ and $g_{9/2}$ orbitals
  same ordering as CC calculations

- reduction of the $\nu d_{3/2}$-$f_{7/2}$ gap with removing $d_{5/2}$ protons
- proximity of the quasi-SU3 partner $p_{3/2}$
- inversion of $p_{3/2}$ and $f_{7/2}$ orbitals

Neutron effective single particle energies

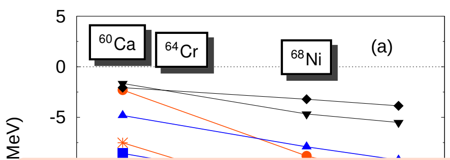

PRL **109,** 032502 (2012)

TABLE II. Energies of the $5/2^+$ and $9/2^+$ resonances in ^{53,55,61}Ca. Re[E] is the energy relative to the one-neutron emission threshold, and the width is $\Gamma = -2\text{Im}[E]$ (in MeV).

	^{53}Ca		^{55}Ca		^{61}Ca	
J^π	Re[E]	Γ	Re[E]	Γ	Re[E]	Γ
$5/2^+$	1.99	1.97	1.63	1.33	1.14	0.62
$9/2^+$	4.75	0.28	4.43	0.23	2.19	0.02

G. Hagen et al.

Phys. Rev. Lett. **109**, 032502 (2012)

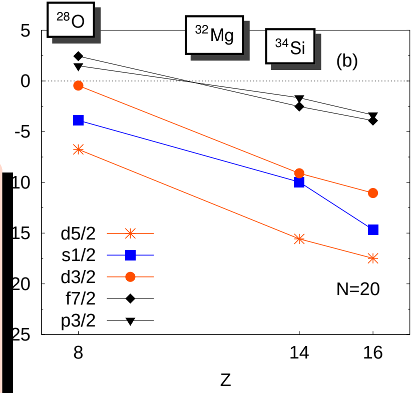

- removing $f_{7/2}$ protons
- proximity of the quasi-SU3 partner $d_{5/2}$
- inversion of $d_{5/2}$ and $g_{9/2}$ orbitals
  same ordering as CC calculations

- reduction of the $\nu d_{3/2}$-$f_{7/2}$ gap with removing $d_{5/2}$ protons
- proximity of the quasi-SU3 partner $p_{3/2}$
- inversion of $p_{3/2}$ and $f_{7/2}$ orbitals

Spin-orbit shell closure far from stability

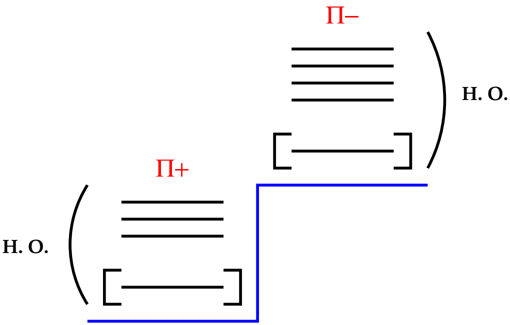

- sd-pf: ^{42}Si deformed
- pf-sdg: ^{78}Ni ???
- sdg-phf: ^{132}Sn doubly magic

- Evolution of Z=28 from N=40 to N=50
- Evolution of N=50 from Z=40 to Z=28

Spin-orbit shell closure far from stability

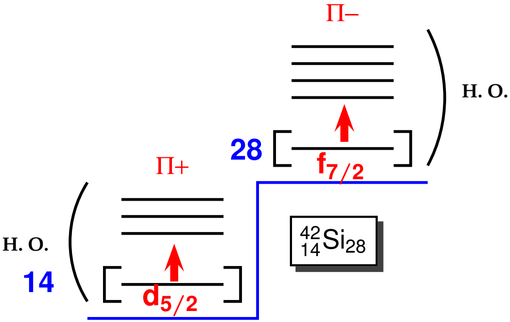

- sd-pf: ^{42}Si deformed
- pf-sdg: ^{78}Ni ???
- sdg-phf: ^{132}Sn doubly magic

- Evolution of Z=14 from N=20 to N=28
- Evolution of Z=28 from N=40 to N=50
- Evolution of N=50 from Z=40 to Z=28

Spin-orbit shell closure far from stability

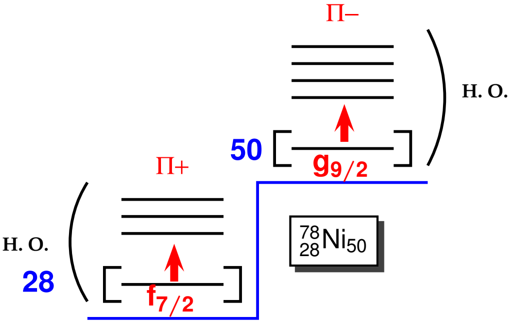

- sd-pf: ^{42}Si deformed
- pf-sdg: ^{78}Ni ???
- sdg-phf: ^{132}Sn doubly magic

- Evolution of Z=14 from N=20 to N=28
- Evolution of Z=28 from N=40 to N=50
- Evolution of N=50 from Z=40 to Z=28

Spin-orbit shell closure far from stability

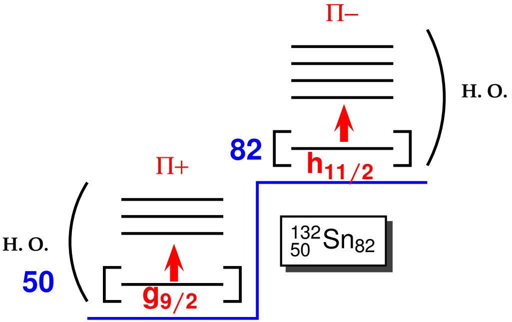

- sd-pf: ^{42}Si deformed
- ^{78}Ni ???
- pf-sdg: sdg-phf: ^{132}Sn doubly magic

- Evolution of Z=14 from N=20 to N=28
- Evolution of Z=28 from N=40 to N=50
- Evolution of N=50 from Z=40 to Z=28

Physics around ^{78}Ni

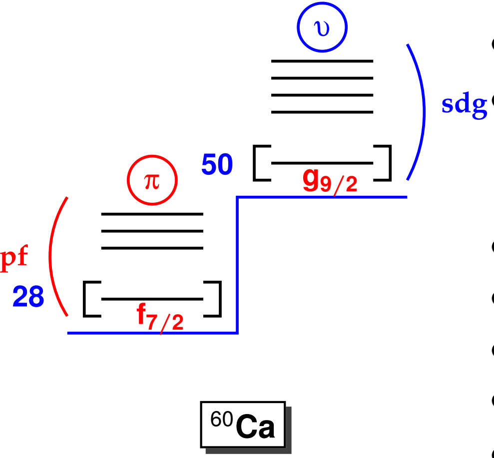

PFSDG-U interaction:

- realistic TBME
- pf shell for protons and gds shell for neutrons
- monopole corrections (3N forces)
- proton and neutrons gap ^{78}Ni fixed to phenomenological derived values

Calculations:

- excitations across Z=28 and N=50 gaps
- up to $5*10^{10}$ Slater Determinant basis states
- up to $3*10^{13}$ non-zero terms in the matrix!
- m-scheme code ANTOINE (non public version)
- J-scheme code NATHAN (parallelized version): $0.5*10^9$ J basis states

Physics around ^{78}Ni

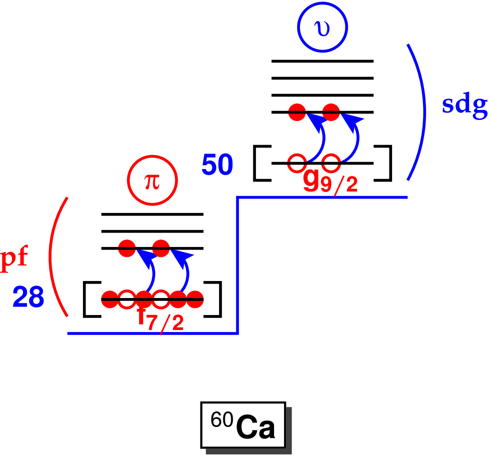

PFSDG-U interaction:

- realistic TBME
- pf shell for protons and gds shell for neutrons
- monopole corrections (3N forces)
- proton and neutrons gap ^{78}Ni fixed to phenomenological derived values

Calculations:

- excitations across Z=28 and N=50 gaps
- up to $5*10^{10}$ Slater Determinant basis states
- up to $3*10^{13}$ non-zero terms in the matrix!
- m-scheme code ANTOINE (non public version)
- J-scheme code NATHAN (parallelized version): $0.5*10^{9}$ J basis states

Shape coexistence in ^{78}Ni

- At first approximation, ^{78}Ni has a double closed shell structure for GS
- But very low-lying competing structures
- From the diagonalization, the first excited states in ^{78}Ni are :
  • 0_2^+-2_1^+ predicted at 2.6-2.9 MeV and to be deformed intruders of a **rotationnal band** !!!
- "$1p1h$" 2_2^+ predicted at $\sim$ 3.1 MeV
- Necessity to go **beyond** ($fpg_{\frac{9}{2}}d_{\frac{5}{2}}$) **LNPS space** and **beyond ab-initio description**
- Portal to a new **I**sland **o**f **I**nversion

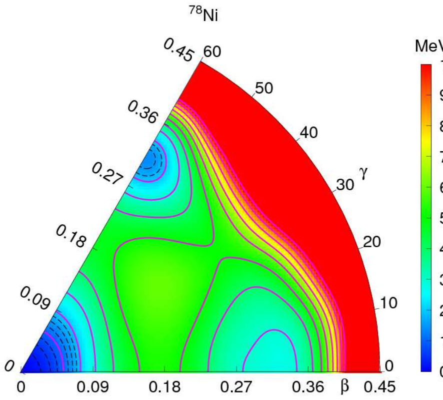

Constrained deformed HF in the SM basis

(Duy Duc Dao, DNO-SM calc., Strasbourg)

Shape coexistence in ^{78}Ni

- At first approximation, ^{78}Ni has a double closed shell structure for GS
- But very low-lying competing structures
- From the diagonalization, the first excited states in ^{78}Ni are :
  • 0_2^+-2_1^+ predicted at 2.6-2.9 MeV and to be deformed intruders of a **rotationnal band** !!!
- "1p1h" 2_2^+ predicted at $\sim$ 3.1 MeV
- Necessity to go **beyond** ($fpg_{\frac{9}{2}}d_{\frac{5}{2}}$) **LNPS space** and **beyond ab-initio description**
- Portal to a new **I**sland **o**f **I**nversion
  F. Nowacki et al., PRL **177**, 272501 (2016)

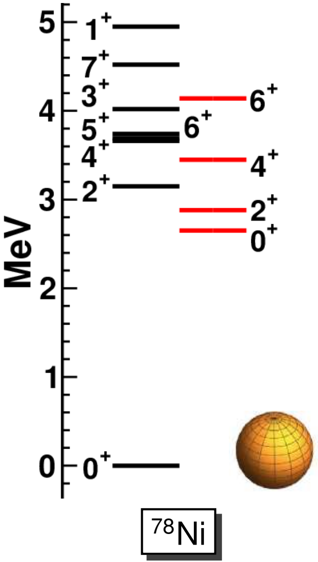

Shape coexistence in ^{78}Ni

- At first approximation, ^{78}Ni has a double closed shell structure for GS
- But very low-lying competing structures
- From the diagonalization,
  the first excited states in ^{78}Ni are :
  • 0_2^+-2_1^+ predicted at 2.6-2.9 MeV and to be deformed intruders of a **rotationnal band** !!!
- "1*p*1*h*" 2_2^+ predicted at $\sim$ 3.1 MeV
- Necessity to go **beyond** ($fpg_{\frac{9}{2}}d_{\frac{5}{2}}$) **LNPS space** and **beyond ab-initio description**
- Portal to a new **I**sland **o**f **I**nversion
  F. Nowacki et al., PRL **177**, 272501 (2016)

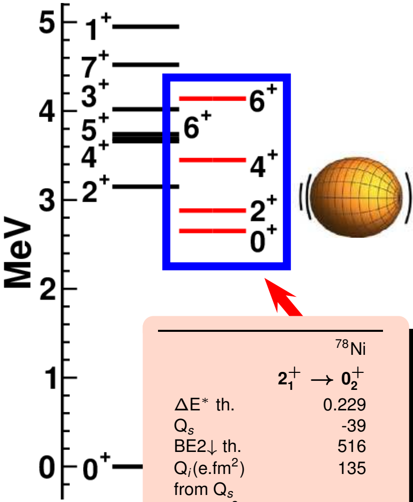

	^{78}Ni
	$\mathbf{2_1^+ \rightarrow 0_2^+}$
ΔE^* th.	0.229
Q_s	-39
BE2↓ th.	516
Q_i(e.fm^2) from Q_s	135
Q_i(e.fm^2) from BE2	195
β_2^e	$\sim$ **0.3 prolate**

Shape coexistence in ^{78}Ni

- At first approximation, ^{78}Ni has a double closed shell structure for GS
- But very low-lying competing structures
- From the diagonalization, the first excited states in ^{78}Ni are :
  • 0_2^+-2_1^+ predicted at 2.6-2.9 MeV and to be deformed intruders of a **rotationnal band** !!!
- "1*p*1*h*" 2_2^+ predicted at $\sim$ 3.1 MeV
- Necessity to go **beyond** ($fpg_{\frac{9}{2}}d_{\frac{5}{2}}$) **LNPS space** and **beyond ab-initio description**
- Portal to a new **I**sland **o**f **I**nversion
  F. Nowacki et al., PRL **177**, 272501 (2016)

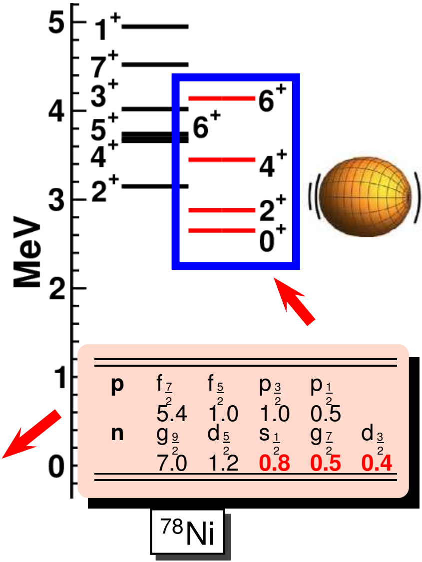

Shape coexistence in ^{78}Ni

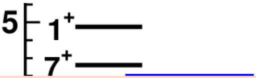

- At first approximation, ^{78}Ni has a double

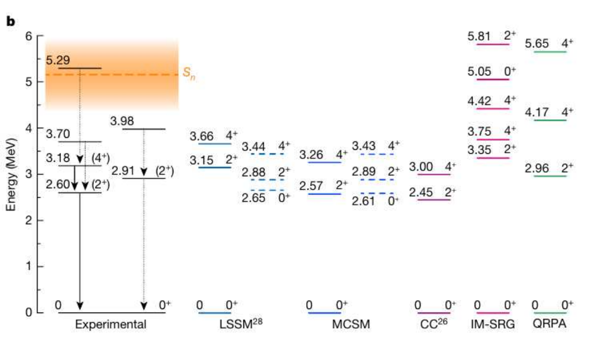

R. Taniuchi et al., NATURE 569, 53-58 (2019)

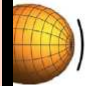

$d_{\frac{3}{2}}$
0.4

F. Nowacki et al., PRL **177**, 272501 (2016)

^{78}Ni

Shape coexistence in ^{78}Ni

- At first approximation, ^{78}Ni has a double

ARTICLE

https://doi.org/10.1038/s41586-019-1155-x

^{78}Ni revealed as a doubly magic stronghold against nuclear deformation

R. Taniuchi[1,2], C. Santamaria[2,3], P. Doornenbal[2*], A. Obertelli[2,3,4], K. Yoneda[2], G. Authelet[3], H. Baba[2], D. Calvet[3], F. Château[3], A. Corsi[3], A. Delbart[3], J.-M. Gheller[3], A. Gillibert[3], J. D. Holt[5], T. Isobe[2], V. Lapoux[3], M. Matsushita[6], J. Menéndez[6], S. Momiyama[1,2], T. Motobayashi[2], M. Niikura[1], F. Nowacki[7], K. Ogata[8,9], H. Otsu[2], T. Otsuka[1,2,6], C. Péron[3], S. Péru[10], A. Peyaud[3], E. C. Pollacco[3], A. Poves[11], J.-Y. Roussé[3], H. Sakurai[1,2], A. Schwenk[4,12,13], Y. Shiga[2,14], J. Simonis[4,12,15], S. R. Stroberg[5,16], S. Takeuchi[2], Y. Tsunoda[6], T. Uesaka[2], H. Wang[2], F. Browne[17], L. X. Chung[18], Z. Dombradi[19], S. Franchoo[20], F. Giacoppo[21], A. Gottardo[20], K. Hadyńska-Klęk[21], Z. Korkulu[19], S. Koyama[1,2], Y. Kubota[2,6], J. Lee[22], M. Lettmann[4], C. Louchart[4], R. Lozeva[7,23], K. Matsui[1,2], T. Miyazaki[1,2], S. Nishimura[2], L. Olivier[20], S. Ota[6], Z. Patel[24], E. Şahin[21], C. Shand[24], P.-A. Söderström[2], I. Stefan[20], D. Steppenbeck[6], T. Sumikama[25], D. Suzuki[20], Z. Vajta[19], V. Werner[4], J. Wu[2,26] & Z. Y. Xu[22]

R. Taniuchi et al., NATURE 569, 53-58 (2019)

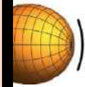

$d_{\frac{3}{2}}$

0.4

- Portal to a new island of inversion
  F. Nowacki et al., PRL **177**, 272501 (2016)

^{78}Ni

Island of Inversion Mergers

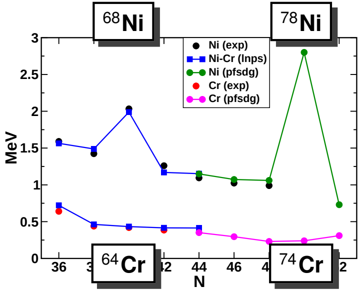

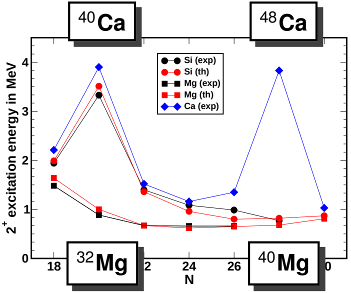

Island of Inversion Mergers

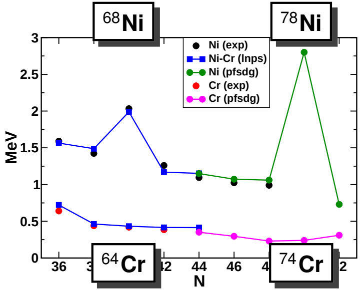

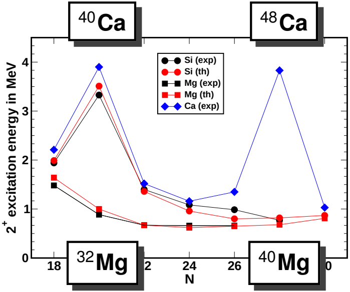

The N=40 and N=50 IoI's merge like the N=20 and N=28 IoI's did

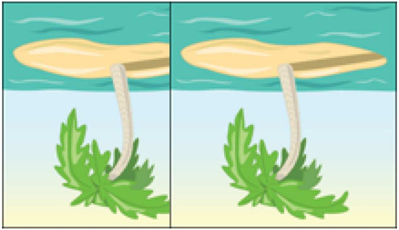

Landscape of medium mass nuclei

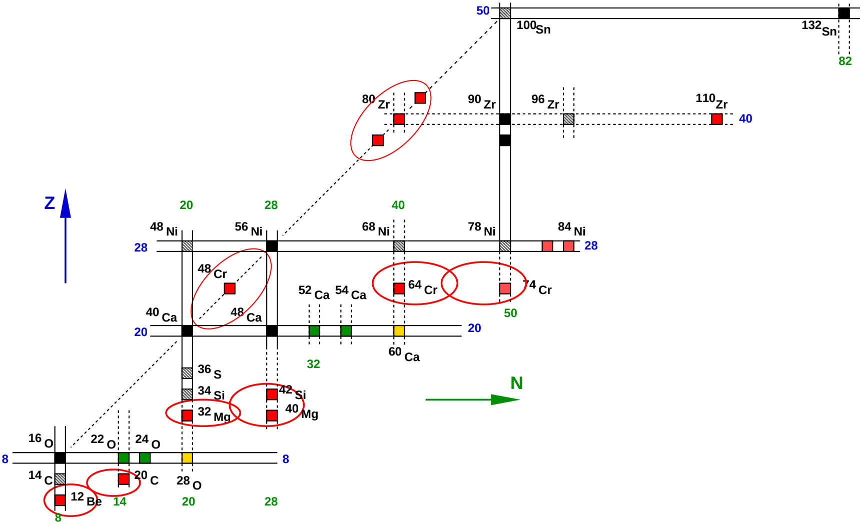

Island of Inversion at the N=Z line

◇ Strongly deformed states at $N = Z$:

- Configuration mixing in ^{72}Kr
- Most deformed cases for ^{76}Sr, ^{80}Zr
- Shape transition between ^{84}Mo and ^{86}Mo
  NSCL/GRETINA Experiment

R.D.O. Llewellyn *et al.*, Phys. Rev. Lett. **124**, 152501 (2020)

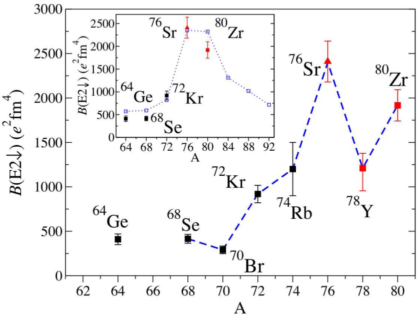

FIG. 3. Schematics of the $B(E2\downarrow)$ values for the $N = Z$ nuclei

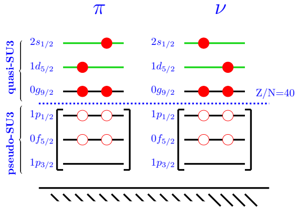

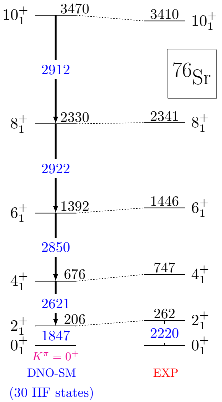

Island of Inversion at the N=Z line

◇ Strongly deformed states at $N = Z$

- Configuration mixing in ^{72}Kr
- Most deformed cases for ^{76}Sr, ^{80}Zr
- Shape transition between ^{84}Mo and ^{86}Mo
  NSCL/GRETINA Experiment

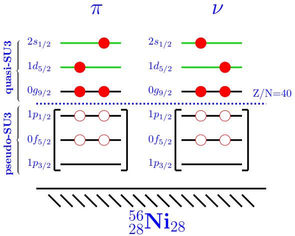

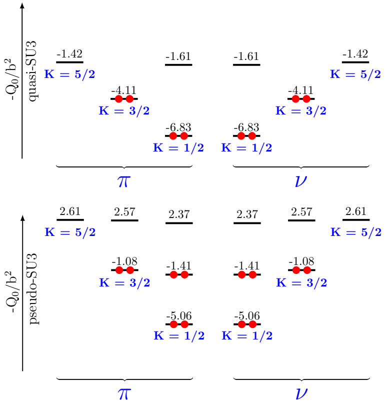

				B(E2)(e^2.fm^4)	
nucleus	NpNh*	ZRP	PHF	DNO-SM	Exp.
^{76}Se	4p-4h	924	806	1847	2220
	8p-8h	2189	2101		
	12p-12h	2316	-		
^{80}Zr	4p-4h	587	637	2325	1910
	8p-8h	1713	1509		
	12p-12h	2663	2396		

Island of Inversion at the N=Z line

◇ Strongly deformed states at $N = Z$

- Configuration mixing in ^{72}Kr
- Most deformed cases for ^{76}Sr, ^{80}Zr
- Shape transition between ^{84}Mo and ^{86}Mo
  NSCL/GRETINA Experiment

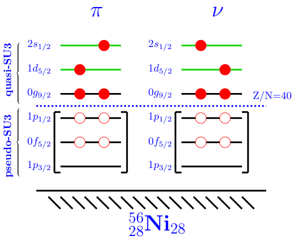

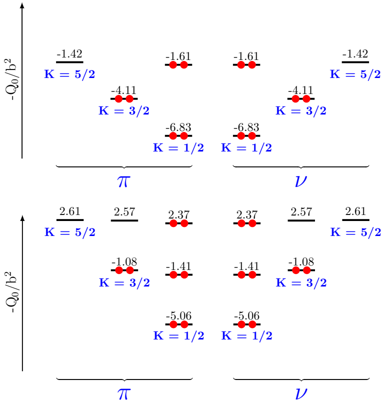

			B(E2)($e^2.fm^4$)			
nucleus	Np-Nh*	ZRP	PHF	DNO-SM*	SM	Exp.
^{84}Mo	4p-4h 8p-8h	1104 1891	1193 1732	1765	-	1740^{+580}_{-730}
^{86}Mo	0p-0h 2p-2h 4p-4h 6p-6h	542 1030 1416 1858	196 871 1179 1655	1184	731	707(71)

Island of Inversion at the N=Z line

- ◇ Strongly deformed states at $N = Z$
  - Configuration mixing in ^{72}Kr
  - Most deformed cases for ^{76}Sr, ^{80}Zr
  - Shape transition between ^{84}Mo and ^{86}Mo

    NSCL/GRETINA Experiment

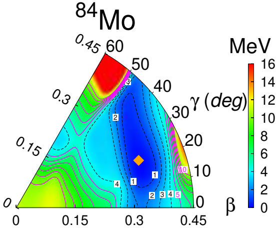

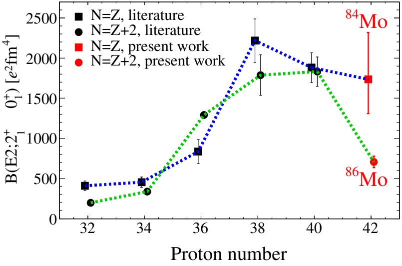

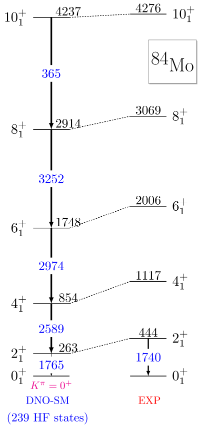

J. Ha, F. Recchia *et al.*, submitted

Island of Inversion at the N=Z line

◇ Strongly deformed states at $N = Z$

- Configuration mixing in ^{72}Kr
- Most deformed cases for ^{76}Sr, ^{80}Zr
- Shape transition between ^{84}Mo and ^{86}Mo

NSCL/GRETINA Experiment

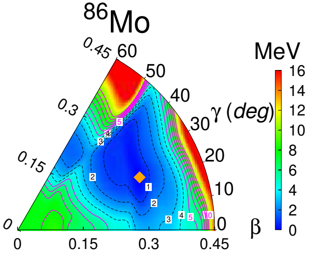

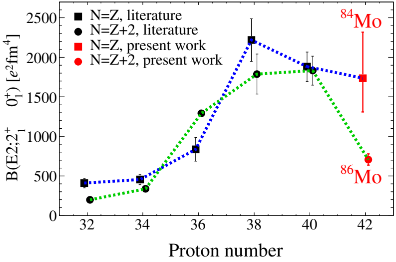

nucleus	Np-Nh*	ZRP	PHF	B(E2)(e^2.fm^4) DNO-SM*	SM	Exp.
^{84}Mo	4p-4h	1104	1193	1765	-	1740^{+580}_{-730}
	8p-8h	1891	1732			
^{86}Mo	0p-0h	542	196	1184	731	707(71)
	2p-2h	1030	871			
	4p-4h	1416	1179			
	6p-6h	1858	1655			

J. Ha, F. Recchia *et al.*, submitted

Island of Inversion at the N=Z line

◇ Strongly deformed states at $N = Z$

- Configuration mixing in ^{72}Kr
- Most deformed cases for ^{76}Sr, ^{80}Zr
- Shape transition between ^{84}Mo and ^{86}Mo

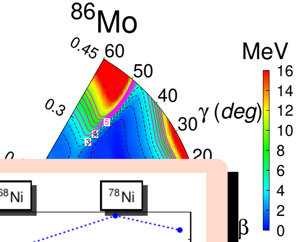

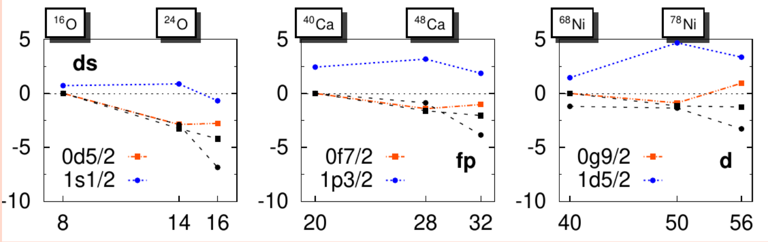

K. Sieja, F. Nowacki

Phys. Rev. **C85**, 051301(R) (2012)

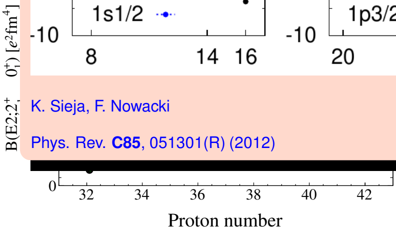

		SM	Exp.
		-	1740^{+580}_{-730}
		731	707(71)
6p-6h	1858	1655	

J. Ha, F. Recchia *et al.*, submitted

Summary

- Monopole drift develops in all regions but the Interplay between correlations (pairing + quadrupole) and spherical mean-field (monopole field) determines the physics.
  It can vary from :
  - island of deformation at N=20 and N=40
  - deformation at Z=14, N=28 for ^{42}Si and shell weakening at Z=28, N=50 for ^{78}Ni

- The “islands of inversion” appear due to the effect of the correlations, hence they could also be called “islands of enhanced collectivity”. As quadrupole correlations are dominant in this region, most of thei inhabitants are deformed rotors. Shape transitions and coexistence show up everywhere

- Quadrupole energies can be huge and understood in terms of symmetries

Summary

- even at the drip in fluorine isotopes, bound approximation holds
- strong superfluid regime with pair scattering from sd to pf shells
- odd-even Sn energies staggering does not seem to originate from continuum coupling

Special thanks to:

- D. D. Dao, G. Martinez-Pinedo, A. Poves, S. Lenzi, K. Sieja
- A. Gade, O. Sorlin, A. Obertelli
- J. Herzfeld-Nowacki